Control of the Carrier Type in InAs Nanocrystal Films by Predeposition Incorporation of Cd

Scott M. Geyer,[†] Peter M. Allen,[†] Liang-Yi Chang,[†] Cliff R. Wong,[†] Tim P. Osedach,[‡] Ni Zhao,[‡] Vladimir Bulovic,[‡] and Moungi G. Bawendi[†,*]

[†]Department of Chemistry and [‡]Department of Electrical Engineering and Computer Science, Massachusetts Institute of Technology, 77 Massachusetts Avenue, Cambridge, Massachusetts 02139, United States

ABSTRACT Nanocrystal (NC) films have been proposed as an alternative to bulk semiconductors for electronic applications such as solar cells and photodetectors. One outstanding challenge in NC electronics is to robustly control the carrier type to create stable p—n homojunction-based devices. We demonstrate that the postsynthetic addition of Cd to InAs nanocrystals switches the resulting InAs:Cd NC films from n-type to p-type when operating in a field effect transistor. This method presents a stable, facile way to control the carrier type of InAs nanocrystals prior to deposition. We present two mechanisms to explain the observed switch in carrier type. In mechanism 1, Cd atoms are incorporated at In sites in the lattice and act as acceptor defects, forming a partially compensated p-type semiconductor. In mechanism 2, Cd atoms passivate donor-type InAs surface states and create acceptor-type surface states. This work represents a critical step toward the creation of p—n homojunction-based NC electronics.

KEYWORDS: nanocrystal · quantum dot · InAs · photoconductivity

The ability to control the carrier type and concentration in bulk semiconductors with high spatial resolution is of fundamental importance for device fabrication. In contrast, the functioning of the majority of semiconductor nanocrystal (NC)-based devices is dictated by the intrinsic carrier density as determined by NC surface states. For example, in the case of lead chalcogenide NC-based Schottky junction solar cells, the barrier height and depletion region are determined by the hole carrier density, which can be altered by changes to the surface chemistry such as oxidation.[1−3] The ability to control carrier type *via* the addition of stable donor or acceptor states to nanocrystals has been a longstanding challenge.[4]

The addition of charge carriers to nanocrystal films has been realized by several distinct methods.[5−9] Direct charge addition has been accomplished through cyclic voltametry.[8,9] Sodium biphenyl has been used to introduce electrons into CdSe NCs, but the nanocrystals are quickly oxidized, which removes the electron.[5,10] Hydrazine postdeposition treatments have been used to switch the conduction of PbSe NC films from p-type to n-type, with the materials reverting to p-type conduction when the hydrazine desorbs from the surface.[6] Binary superlattices have been employed to remotely dope PbTe.[7] However, a stable predeposition method to control the carrier type in NCs has yet to be reported.

In this work, we demonstrate the ability to switch InAs NC films from n-type to p-type conduction through the incorporation of Cd. Cd is a stable transition metal cation that can be added to the InAs NCs prior to deposition. Films of InAs:Cd NCs demonstrate fundamentally different dark and photoconductive properties than InAs NC films, indicating that the incorporation of Cd has a large effect on the density of states within the band gap. We also investigate InAs/CdZnSe core/shell NCs, where the III−V core is surrounded by a shell of II−VI atoms which passivate the surface and may act as donors and acceptors if incorporated into the III−V lattice. We find that films of InAs/CdZnSe NCs exhibit ambipolar conduction when gated after annealing. The ability to switch carrier type using a stable predeposition dopant is an essential step toward the creation of p−n junction nanocrystal solar cells and other homojunction-based nanocrystal devices.

RESULTS AND DISCUSSION

Bulk InAs has been shown to have an n-type surface accumulation region due to electron-donating surface states.[11] For high surface area nanostructures, such as InAs nanowires, this results in inherent n-type conduction.[12] These surface states also lead to a large amount of Fermi level pinning at the metal contact, causing InAs to form

*Address correspondence to mgb@mit.edu.

Received for review July 26, 2010 and accepted November 22, 2010.

Published online December 2, 2010.
10.1021/nn101772n

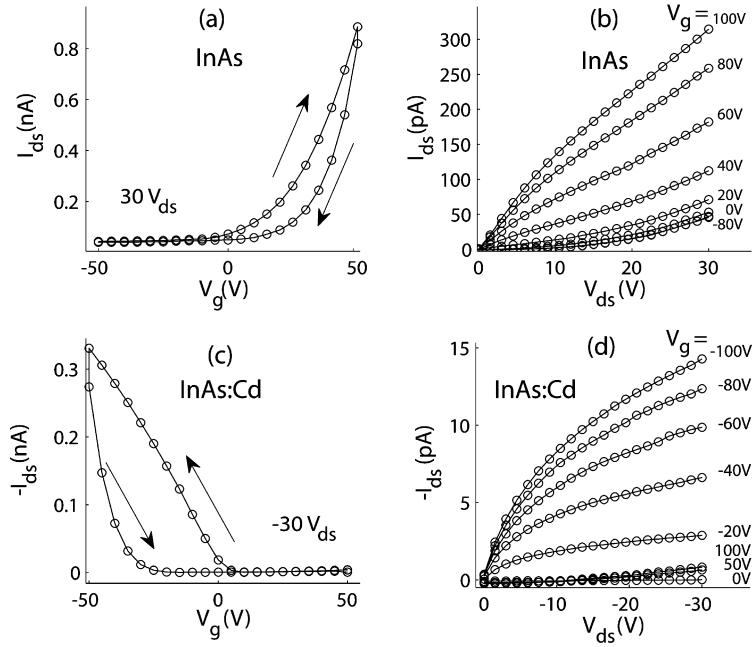

Figure 1. (a) Dependence of source−drain current on gate voltage for InAs NC films showing n-type behavior. (b) Output curves from the same InAs device. (c) Transfer curve for InAs:Cd NC films showing p-type behavior. (d) Output curves from the same InAs:Cd device.

ohmic contacts with many metals including gold.[13] Sulfur passivation or thiol treatment has been shown to reduce contact resistance and improve mobility in InAs nanowires.[12] This is attributed to the reduction in the number of surface trap states.[12] For these reasons, ethanedithiol is chosen as the ligand for postdeposition ligand exchange treatment for all of the NC systems in this work.[14−16]

The gate dependence of nanocrystal films in a field effect transistor (FET) is commonly used to determine the film carrier type.[2,6,17,18] The gate dependence and output curves of InAs core NC films are shown in Figure 1a,b, respectively. The InAs channel is n-type with clear hysteresis indicating trapping of the added charge. To reduce hysteresis, the gate voltage is pulsed to the measurement value and then back to zero between each data point.[17,19] The NC film is on SiOx, which is known to have electron acceptors at the surface, and is therefore unlikely to give rise to the observed n-type behavior, suggesting this is a property of the NC film. The observed n-type conduction is in agreement with previous reports on the surfaces of bulk InAs[11] and InAs nanowires.[12] The positive threshold voltage is consistent with the filling of midgap trapping states which may give rise to the observed hysteresis. At low and negative gate voltages, the output curves are supralinear. Supralinear conduction is commonly observed in nanocrystal films.[2,17,20] At higher gate voltages, the source−drain current increases sublinearly with voltage as the FET nears the saturation regime.

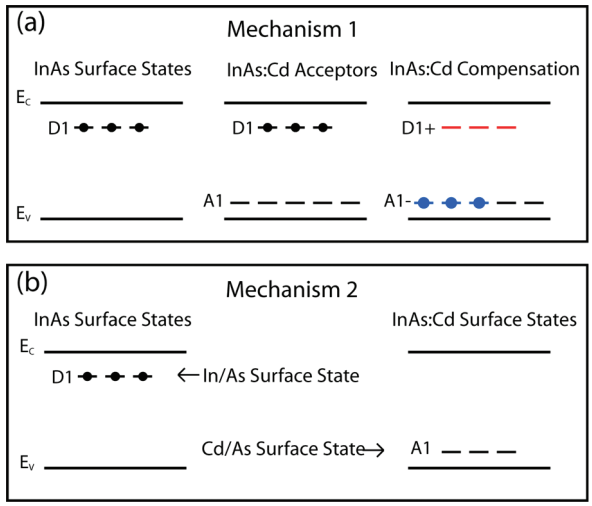

Figure 2. Cartoon depiction of mechanisms for p-type doping of InAs:Cd nanocrystals. In mechanism 1, the addition of acceptors by Cd over compensates the electron donors on the surface, leading to a partially compensated semiconductor. In mechanism 2, the surface states are altered by the addition of a monolayer of Cd.

InAs:Cd NC films are prepared identically to the InAs core NC films, as described in the Methods section. Figure 1c shows the effect of the gate voltage on the source−drain current, and Figure 1d shows output curves for the same device. A switch to p-type conduction is observed. For both InAs and InAs:Cd NC films, the same gold contacts are used. The observation of n-type conduction in InAs NC films indicates that it is possible to inject electrons from the gold contacts into the NC film. The p-type conduction in InAs:Cd NC films similarly indicates that hole injection from the electrodes is possible. Therefore, the observed n-type and p-type behavior is attributed to the carrier type of the NC film, rather than the presence of blocking contacts for either electrons or holes. A larger amount of hysteresis is observed in the InAs:Cd films, indicating that holes are trapped more quickly or more deeply in InAs:Cd NC films than electrons in InAs NC films.

The switch of majority carrier from electrons to holes is due to acceptor states generated by the Cd incorporated into the NCs. We present two mechanisms to explain the observed behavior. In mechanism 1 (Figure 2a), Cd occupies an In lattice position (Cd_{In}) as a substitutional impurity. Cd assumes the same bonding configuration as In in the lattice but due to its lower number of valence electrons creates an acceptor state impurity. Diffusion doping of bulk InAs has previously been accomplished using Cd_3As_2,[21] which like $Cd(oleate)_2$ introduces the Cd into the lattice in a +2

oxidation state. The diffusion constant of Cd in bulk InAs at 300 °C is 5.9×10^{-14} cm^2/s.[22,23] Therefore, the diffusion length will be longer than the nanocrystal diameter even if the diffusion constant of Cd in the nanocrystal is 3 orders of magnitude lower than the bulk value. Substitutional incorporation of an impurity atom in a nanocrystal has previously been shown with EPR studies on Mn-doped CdSe.[24] Cadmium[25] and zinc[26] doping of InAs nanowires has been demonstrated. Incorporation of copper into In_2S_3 NCs has also been reported.[27] In mechanism 1, the switch from n-type to p-type conduction does not require the added Cd to quench all of the donor sites (D1) on the InAs surface. Instead, the Cd acceptor states (A1) overcompensate the intrinsic donors, so that the number of acceptors is greater than the number of donors, $N_A > N_D$. At thermal equilibrium, the donor electrons reside in negatively charged filled acceptor states (A1−), which act as hole traps, leaving behind positively charged empty donor states which can act as recombination centers for photoexcited electrons (D1+). In mechanism 2 (Figure 2b), Cd atoms bound to the surface passivate the InAs donor state and create an acceptor state. For PbS and CdTe NCs, acceptor states have been associated with multiatom surface constructs such as $PbSO_3$ and $PbSO_4$ for PbS NCs[18] and TeO_2 and $CdTeO_3$ for CdTe NCs.[28] As suggested for Cd-doped InAs nanowires,[25] the change from n-type to p-type may be a combination of mechanisms 1 and 2, where surface state passivation lowers the number of donor states and substitutional impurities create acceptor states.

In this work, we refer to the NC *film* carrier type, rather than the NC carrier type, to distinguish that we are measuring the property of a large number of nanocrystals that have undergone specific chemical treatments. The NC solution contains individual NCs that vary in composition and defect states, and therefore, it is misleading to assign a carrier type to the NC solution. However, the properties of the NC film are governed by the overall distribution of defect states present, which can be altered prior to deposition, allowing for control over the film carrier type.

InAs:Cd NCs were characterized by absorption spectroscopy, energy-dispersive X-ray spectroscopy (EDS), and inductively coupled plasma atomic emission spectroscopy (ICP-AES). EDS and ICP-AES are used to determine the amount of Cd present in the purified InAs:Cd NCs and give relative concentrations of In:As:Cd of 2.0:2.2:1.0 and 1.9:2.4:1, respectively (Figure 3a). On the basis of the lattice constant of InAs and the 4 nm diameter of the NCs, we estimate that there are ~600 In and ~600 As atoms per NC. A monolayer of Cd atoms on the surface of the NC would add ~320 Cd atoms and would result in a relative concentration of In:As:Cd of 1.9:1.9:1, in good agreement with the observed ratios.

The absorption spectra of InAs NC and InAs:Cd NC made from the same synthesis are shown in Figure 3b.

(a)

Relative Composition of InAs:Cd by Number of Atoms

Type of Analysis	In	As	Cd
EDS	2.0	2.2	1.0
ICP-AES	1.9	2.4	1.0
Calculation for Monolayer of Cd	1.9	1.9	1.0

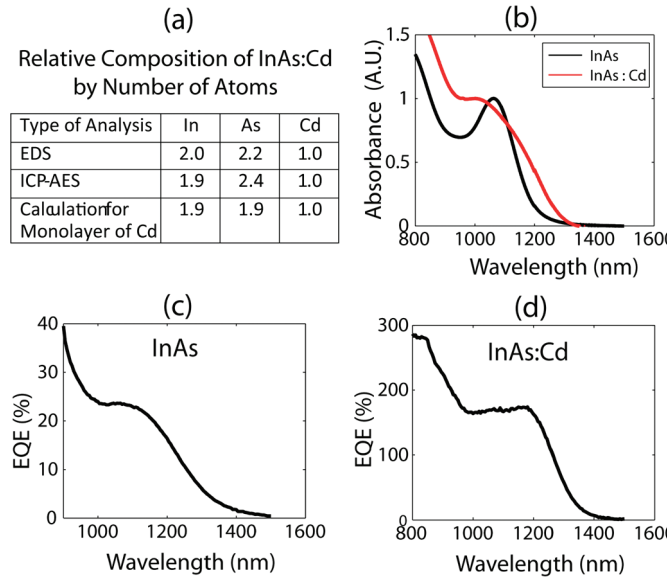

Figure 3. (a) EDS and ICP-AES composition analysis compared to the estimated composition for a monolayer of Cd absorbed to the surface. (b) Absorption spectra of InAs and InAs:Cd showing retention of the InAs feature after synthesis of InAs:Cd. (c,d) Photoaction spectra for InAs and InAs:Cd devices on quartz demonstrating that confinement is retained in the NC films.

The InAs:Cd NC 1S transition absorption feature broadens and shifts slightly to the red after Cd addition. If there was significant cation exchange and formation of an InCdAs alloy, it is unlikely the spectrum would remain consistent given that the band gap of Cd_3As_2 is 0.14 eV, less than half that of InAs (0.36 eV).[29] The photoaction spectra of InAs and InAs:Cd NC films are shown in Figure 3c,d, respectively. The photoaction spectra demonstrate that the nanocrystals retain their confinement properties in the NC films after processing and ligand exchange. The red shift in the photoaction spectrum relative to the solution phase absorption spectrum is due to the higher dielectric constant in the film.[30] For InAs:Cd nanocrystals, an external quantum efficiency greater than 100% is observed, indicating that gain greater than unity is occurring in these films.

The comparison of the temperature dependence of the photocurrent and dark current between InAs and InAs:Cd NC thin films demonstrates the effect of Cd incorporation on the conduction properties of the film. All temperature dependence data are taken on quartz substrates with films prepared identically to the corresponding field effect transistors. Figure 4a shows the dark current of an InAs NC film plotted *versus* temperature for several voltages. Various mechanisms have been proposed for charge transport in nanocrystal films. We find our data to be best described by the model proposed for CdTe NC films.[17] Similar to CdTe, InAs NC films exhibit a voltage-assisted Arrhenius activation of the dark current. The increase in the dark current is caused by a simultaneous increase in the mobility and the carrier density. The photocurrent, which is proportional to the mobility, increases only by a factor

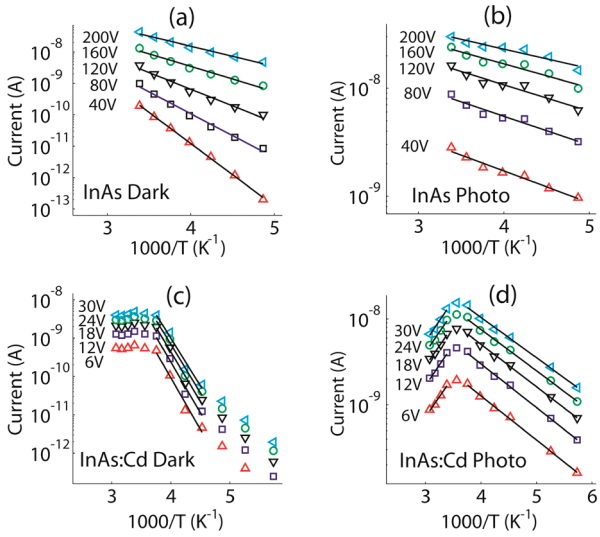

Figure 4. Temperature dependence of InAs dark current (a) and photocurrent (b) compared to InAs:Cd dark current (c) and photocurrent (d). NC films are measured on a quartz substrate with gold electrodes. InAs:Cd NC films show qualitatively different temperature characteristics from InAs, indicating a change in the population of mid gap states.

of 2 over the same temperature region as the dark current increases by 3 orders of magnitude. Therefore, the increased carrier density due to thermal activation dominates the dark current in this temperature range. Fitting to a simple Arrhenius activation model at different voltages, we find a strong voltage dependence on the effective activation energy. The voltage dependence derives, for the case of an n-type NC film, from the lowering of the conduction band of the neighboring nanocrystal relative to the energy of the electron-donating gap state due to the electric field. This voltage-assisted activation mechanism is modeled by eq 1, which gives a relationship between the effective activation energy, ΔE_0, the activation distance, a, and the applied electric field, E.

$$I_{dark} = \frac{E}{\rho_0}\exp\left(\frac{E}{E_0} + \frac{aE - \Delta E_0}{kT}\right) \quad (1)$$

Here ρ_0 is the intrinsic temperature-independent resistivity of the film and E_0 is an empirically derived value that accounts for the supralinear current−voltage characteristics of both the dark current and photocurrent. Fitting the InAs data to eq 1 gives an activation energy of 350 meV and an activation length of 2.4 nm (see Supporting Information). The activation length is on the order of the interparticle spacing, consistent with the values obtained for CdTe. The activation energy reveals the energy of the closest electrons to the conduction band and gives a measure of the position of the Fermi level in the band gap. When the dark current activation for InAs and InAs:Cd at higher temperatures is compared, the dark current in the InAs NC films continues to increase while the current saturates for the InAs:Cd samples. This saturation is attributed to complete ionization of the Cd acceptor states.

Figure 4b,d shows the temperature dependence of the photocurrent for InAs and InAs:Cd, respectively. For InAs, the photocurrent increases with temperature. This is due to thermal activation of electrons out of shallow trap states. As the temperature is increased, the detrapping time is reduced, increasing the effective mobility by increasing the fraction of free carriers.[31] For InAs:Cd, clear temperature-dependent quenching of the photocurrent is observed at higher temperature. This photocurrent quenching is explained by the standard model for thermal quenching of a photosensitizing center.[31] In this model, the gain of a photoconductor decreases with increasing temperature as the minority carrier is thermally excited out of a recombination center. This gives rise to an Arrhenius decay in the photocurrent with increasing temperature. Fitting the photocurrent in the quenching region (see Supporting Information), we determine an activation energy between 110 and 170 meV.

The third InAs-based NC system studied is annealed films of InAs/CdZnSe core/shell NCs. In order to improve photoluminescence properties, InAs particles are commonly overcoated with a shell composed of CdZnSe.[32] As-deposited core/shell NC films exhibit reduced conductivity compared to core NC films because the shell increases the core to core tunneling distance. However, thermally annealed CdSe/CdZnSe core/shell NC films with a 2−3 monolayer thick shell have been shown to maintain quantum confinement of the exciton and demonstrate improved photocurrent response over CdSe core NC films.[33]

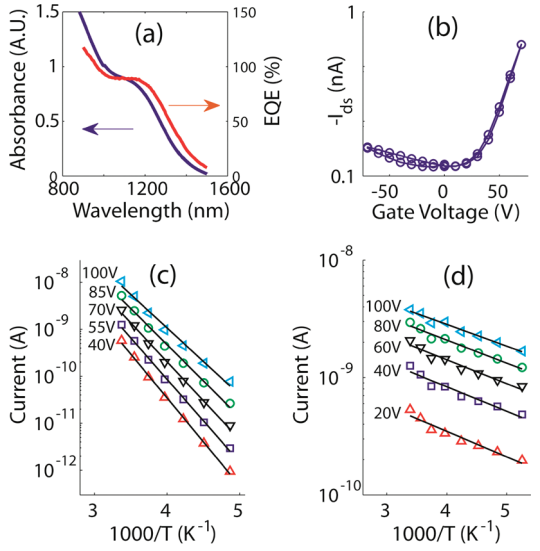

Figure 5. Electrical characteristics of InAs/CdZnSe core/shell NC films annealed at 300 °C. (a) Photoaction spectrum compared to absorption in solution demonstrating confinement of the exciton after annealing. (b) Ambipolar NC film with p-type conduction at zero gate bias. (c) Dark current activation and (d) photocurrent activation curves shown on an Arrhenius plot at different source−drain voltages.

InAs/CdZnSe core/shell NCs are prepared from 4.1 nm cores and overcoated to reach a final size of 5.9 nm as determined by TEM. This is consistent with three monolayers of CdZnSe. Figure 5a shows the photoaction spectrum of an InAs/CdZnSe NC film after annealing at 300 °C under vacuum of 24 Torr for 30 min, compared with the solution phase absorption spectrum. Confinement of the exciton is maintained, and the photocurrent response is similar in magnitude to the core NC films. The transfer curves for a 300 °C annealed NC film (Figure 5b) show ambipolar behavior, with the NC film being p-type at zero bias. The ambipolar behavior indicates that the density of midgap states is low enough that the Fermi level can be raised from near the valence band to near the conduction band by the applied gate voltage, which we attribute to surface passivation by the shell. The dark current temperature dependence shown in Figure 5c fits well to the same model used for InAs NC, with an activation energy of 410 meV and activation length of 1.4 nm. The photocurrent temperature dependence (Figure 5d) resembles that of InAs and does not exhibit a photocurrent quenching regime.

CONCLUSION

We have presented electrical characterization of thin films of InAs, InAs:Cd, and InAs/CdZnSe nanocrystals. In each case, the photoaction spectrum demonstrates that the NC films are photosensitive and retain the quantum confined properties of the NC. Consistent with the bulk and nanowire forms of InAs, InAs NC films exhibit n-type conduction attributed to electron-donating surface states. The incorporation of Cd atoms prior to deposition results in p-type InAs:Cd films. This provides a facile, stable route for controlling carrier type of InAs NCs. We attribute the switch in carrier type to either generation of acceptor states when Cd substitutes for an In site in the NC lattice or creation of acceptor surface states by Cd. Ambipolar behavior is observed in annealed InAs/CdZnSe core/shell NCs. The results presented here motivate further investigation of transition metal impurity incorporation for carrier control in nanocrystal-based electronics.

METHODS

Synthesis. InAs core and InAs/CdZnSe core/shell NCs were synthesized according to published procedures (see Supporting Information).[32,34,35] To synthesize InAs:Cd NCs, a 0.2 M solution of $Cd(oleate)_2$ with oleylamine is prepared by adding 514 mg of CdO, 2.5 mL of oleic acid, and 2.5 mL of oleylamine to 14.8 mL of octadecene. This solution is put under vacuum for 1 h at 100 °C, heated under nitrogen to 280 °C until the reddish CdO tint disappears, and then placed under vacuum for 1 additional hour at 100 °C. Sufficient $Cd(Oleate)_2$ was added to the InAs growth solution to form approximately 1 monolayer of Cd on the surface of the InAs NCs, similar to the SILAR technique for overcoating.[36,37] This solution is heated to 290 °C for 3 h. The results of heating at a lower temperature is discussed in the Supporting Information.

Composition Analysis. Energy-dispersive X-ray spectroscopy (EDS) was conducted with a JEOL 6320FV SEM equipped with an EDS detector. Inductively coupled plasma atomic emission spectroscopy (ICP-AES) is performed with an Activa system from Horiba Scientific. Samples were prepared by dissolving purified nanocrystals in a 3:1 mixture of hydrochloric acid and nitric acid (aqua regia) for 36 h at 75C. Aqua regia was prepared from TraceSelect ultragrade chemicals from Sigma Aldrich to avoid sample contamination.

Film Processing. All NC film deposition and treatment was done in a nitrogen-filled glovebox. Nanocrystals were purified from the growth solution according to published procedure with slight modification.[15,17] The nanocrystals are precipitated three times by adding a mixture of ethanol and acetone to the nanocrystal solution and centrifuging. After each precipitation, the NCs were redissolved in hexane and filtered through a 0.1 μm PTFE filter. The NC films were drop cast from a 10:1 hexane/octane mixture. Postdeposition ligand exchange was done with 100:1 volume ratio of acetonitrile and ethanedithiol for 30 min, after which the NC films were rinsed with pure acetonitrile and baked at 100 °C for 30 min. To fill in cracks created in the NC film during the first treatment, a second layer was drop cast and treated identically to the first layer.[6] For annealing studies, NC films were annealed under vacuum in a nitrogen glovebox. The NC films were held for 30 min at the specified temperature.

Substrates and Measurement. All data were taken using symmetric gold electrodes with a 5 nm chrome adhesion layer. Gold electrodes were deposited prior to nanocrystal deposition. For the photocurrent temperature dependence measurements, a quartz substrate was used. The electrode width was 800 μm, the height was 200 nm, and the channel length is as specified in the text. For gate effect measurements, the NC films were deposited on SiOx on a p+-doped Si substrate. Unless otherwise noted, the electrodes were interdigitated fingers. Each interdigitated electrode had 60 channels of 1 mm channel width for a total channel width of 60 mm, a height of 50 nm, a channel length of 10 μm, and a 950 nm SiOx layer.

The dark conduction data were measured with an Ithaco 1211 transimpedance amplifier connected to an Agilent 34401A multimeter. Photocurrent was measured using mechanically chopped (15 Hz) 514 nm laser excitation and a Stanford Research System 830 lock-in amplifier. The NCs were kept under nitrogen or vacuum throughout the synthesis, processing, deposition, and measurement steps.

External quantum efficiency measurements were taken using a Spectra Pro SP2150 equipped with a tungsten lamp to generate monochromatic light. For each spectral region, appropriate long pass filters were used to isolate the monochromatic light. The intensity of light in the visible was measured with a calibrated Newport 818-UV Si photodiode and in the infared with a Newport 818-IR Ge photodiode.

Acknowledgment. This work was supported in part by the NSF-MRSEC Program (DMR-0819762), making use of its Shared Experimental Facilities, the U.S. Army through the Institute for Soldier Nanotechnologies (W911NF-07-D-004), and the Department of Energy (DE-FG36-08G018007). S.G. acknowledges support from the Corning Foundation and the Martin Family Society.

Supporting Information Available: Nanocrystal synthesis, additional dark current activation curves, photocurrent fitting model, photoquenching data and fitting. This material is available free of charge *via* the Internet at http://pubs.acs.org.

REFERENCES AND NOTES

1. Luther, J. M.; Law, M.; Beard, M. C.; Song, Q.; Reese, M. O.; Ellingson, R. J.; Nozik, A. J. Schottky Solar Cells Based on Colloidal Nanocrystal Films. *Nano Lett.* **2008**, *8*, 3488–3492.
2. Mentzel, T. S.; Porter, V. J.; Geyer, S.; MacLean, K.; Bawendi,

M. G.; Kastner, M. A. Charge Transport in PbSe Nanocrystal Arrays. *Phys. Rev. B* **2008**, *77*, 075316-8.
3. Sargent, E. H. Infrared Photovoltaics Made by Solution Processing. *Nat. Photonics* **2009**, *3*, 325–331.
4. Norris, D. J.; Efros, A. L.; Erwin, S. C. Doped Nanocrystals. *Science* **2008**, *319*, 1776–1779.
5. Shim, M.; Guyot-Sionnest, P. n-Type Colloidal Semiconductor Nanocrystals. *Nature* **2000**, *407*, 981–983.
6. Talapin, D. V.; Murray, C. B. PbSe Nanocrystal Solids for n- and p-Channel Thin Film Field-Effect Transistors. *Science* **2005**, *310*, 86–89.
7. Urban, J. J.; Talapin, D. V.; Shevchenko, E. V.; Kagan, C. R.; Murray, C. B. Synergismin Binary Nanocrystal Superlattices Leads to Enhanced p-Type Conductivity in Self-Assembled PbTe/Ag_2Te Thin Films. *Nat. Mater.* **2007**, *6*, 115–121.
8. Yu, D.; Wang, C. J.; Guyot-Sionnest, P. n-Type Conducting CdSe Nanocrystal Solids. *Science* **2003**, *300*, 1277–1280.
9. Wehrenberg, B. L.; Guyot-Sionnest, P. Electron and Hole Injection in PbSe Quantum Dot Films. *J. Am. Chem. Soc.* **2003**, *125*, 7806–7807.
10. Bang, J.; Chon, B.; Won, N.; Nam, J.; Joo, T.; Kim, S. Spectral Switching of Type-II Quantum Dots by Charging. *J. Phys. Chem. C* **2009**, *113*, 6320–6323.
11. Noguchi, M.; Hirakawa, K.; Ikoma, T. Intrinsic Electron Accumulation Layers on Reconstructed Clean InAs(100) Surfaces. *Phys. Rev. Lett.* **1991**, *66*, 2243.
12. Hang, Q.; Wang, F.; Carpenter, P. D.; Zemlyanov, D.; Zakharov, D.; Stach, E. A.; Buhro, W. E.; Janes, D. B. Role of Molecular Surface Passivation in Electrical Transport Properties of InAs Nanowires. *Nano Lett.* **2007**, *8*, 49–55.
13. Mead, C. A.; Spitzer, W. G. Fermi Level Position at Metal−Semiconductor Interfaces. *Phys. Rev. B* **1964**, *134*, A713.
14. Guyot-Sionnest, P.; Wang, C. Fast Voltammetric and Electrochromic Response of Semiconductor Nanocrystal Thin Films. *J. Phys. Chem. B* **2003**, *107*, 7355–7359.
15. Jarosz, M. V.; Porter, V. J.; Fisher, B. R.; Kastner, M. A.; Bawendi, M. G. Photoconductivity Studies of Treated CdSe Quantum Dot Films Exhibiting Increased Exciton Ionization Efficiency. *Phys. Rev. B* **2004**, *70*, 195327-12.
16. Klem, E. J. D.; MacNeil, D. D.; Cyr, P. W.; Levina, L.; Sargent, E. H. Efficient Solution-Processed Infrared Photovoltaic Cells: Planarized All-Inorganic Bulk Heterojunction Devices *via* Inter-Quantum-Dot Bridging during Growth from Solution. *Appl. Phys. Lett.* **2007**, *90*, 183113-3.
17. Porter, V. J.; Mentzel, T.; Charpentier, S.; Kastner, M. A.; Bawendi, M. G. Temperature-, Gate-, and Photoinduced Conductance of Close-Packed CdTe Nanocrystal Films. *Phys. Rev. B* **2006**, *73*, 155303.
18. Klem, E. J. D.; Shukla, H.; Hinds, S.; MacNeil, D. D.; Levina, L.; Sargent, E. H. Impact of Dithiol Treatment and Air Annealing on the Conductivity, Mobility, and Hole Density in PbS Colloidal Quantum Dot Solids. *Appl. Phys. Lett.* **2008**, *92*, 212105-3.
19. Petit, C.; Zander, D.; Lmimouni, K.; Ternisien, M.; Tondelier, D.; Lenfant, S.; Vuillaume, D. Gate Pulse Electrical Method to Characterize Hysteresis Phenomena in Organic Field Effect Transistor. *Org. Electron.* **2008**, *9*, 979–984.
20. Ginger, D. S.; Greenham, N. C. Charge Injection and Transport in Films of CdSe Nanocrystals. *J. Appl. Phys.* **2000**, *87*, 1361–1368.
21. Horikoshi, Y.; Saito, H.; Takanashi, Y. Simultaneous Diffusion of Zinc and Cadmium into InAs. *Jpn. J. Appl. Phys.* **1981**, *20*, 437.
22. Tuck, B. *Atomic Diffusion in III-V Semiconductors*; Adam Hilger: Bristol, UK, 1988.
23. Madelung, O. *Semiconductors: Group IV Elements and II-V Compounds*; Springer-Verlag: Berlin, 1991; p 139.
24. Beaulac, R.; Archer, P. I.; Ochsenbein, S.; Gamelin, D. R. Mn^{2+}-Doped CdSe Quantum Dots: New Inorganic Materials for Spin-Electronics and Spin-Photonics. *Adv. Funct. Mater.* **2008**, *18*, 3873–3891.
25. Hang, Q.; Wang, F.; Buhro, W. E.; Janes, D. B. Ambipolar Conduction in Transistors Using Solution Grown InAs Nanowires with Cd Doping. *Appl. Phys. Lett.* **2007**, *90*, 062108–062110.
26. Ford, A. C.; Chuang, S.; Ho, J. C.; Chueh, Y.-L.; Fan, Z.; Javey, A. Patterned p-Doping of InAs Nanowires by Gas-Phase Surface Diffusion of Zn. *Nano Lett.* **2010**, *10*, 509–513.
27. Tang, J.; Konstantatos, G.; Hinds, S.; Myrskog, S.; Pattantyus-Abraham, A. G.; Clifford, J.; Sargent, E. H. Heavy-Metal-Free Solution-Processed Nanoparticle-Based Photodetectors: Doping of Intrinsic Vacancies Enables Engineering of Sensitivity and Speed. *ACS Nano* **2008**, *3*, 331–338.
28. Lobo, A.; Borchert, H.; Talapin, D. V.; Weller, H.; Moller, T. Surface Oxidation of CdTe Nanocrystals—A High Resolution Core-Level Photoelectron Spectroscopy Study. *Colloids Surf., A* **2006**, *286*, 1–7.
29. Wei, S.; Lu, J.; Yu, W.; Zhang, H.; Qian, Y. Isostructural Cd_3E_2 (E = P, As) Microcrystals Prepared *via* a Hydrothermal Route. *Cryst. Growth Des.* **2006**, *6*, 849–853.
30. Leatherdale, C. A.; Bawendi, M. G. Observation of Solvatochromism in CdSe Colloidal Quantum Dots. *Phys. Rev. B* **2001**, *63*, 165315.
31. Bube, R. H. *Photoconductivity of Solids*; Wiley: New York, 1960.
32. Aharoni, A.; Mokari, T.; Popov, I.; Banin, U. Synthesis of InAs/CdSe/ZnSe Core/Shell1/Shell2 Structures with Bright and Stable Near-Infrared Fluorescence. *J. Am. Chem. Soc.* **2005**, *128*, 257–264.
33. Porter, V. J.; Geyer, S.; Halpert, J. E.; Kastner, M. A.; Bawendi, M. G. Photoconduction in Annealed and Chemically Treated CdSe/ZnS Inorganic Nanocrystal Films. *J. Phys. Chem. C* **2008**, *112*, 2308–2316.
34. Guzelian, A. A.; Banin, U.; Kadavanich, A. V.; Peng, X.; Alivisatos, A. P. Colloidal Chemical Synthesis and Characterization of InAs Nanocrystal Quantum Dots. *Appl. Phys. Lett.* **1996**, *69*, 1432–1434.
35. Cao, Y.; Banin, U. Growth and Properties of Semiconductor Core/Shell Nanocrystals with InAs Cores. *J. Am. Chem. Soc.* **2000**, *122*, 9692–9702.
36. Xie, R. G.; Kolb, U.; Li, J. X.; Basche, T.; Mews, A. Synthesis and Characterization of Highly Luminescent CdSe-Core CdS/$Zn_{0.5}Cd_{0.5}$S/ZnS Multishell Nanocrystals. *J. Am. Chem. Soc.* **2005**, *127*, 7480–7488.
37. Li, J. J.; Wang, Y. A.; Guo, W.; Keay, J. C.; Mishima, T. D.; Johnson, M. B.; Peng, X. Large-Scale Synthesis of Nearly Monodisperse CdSe/CdS Core/Shell Nanocrystals Using Air-Stable Reagents *via* Successive Ion Layer Adsorption and Reaction. *J. Am. Chem. Soc.* **2003**, *125*, 12567–12575.